Journal of Nuclear Materials 403 (2010) 126–134

Contents lists available at ScienceDirect

Journal of Nuclear Materials

journal homepage: www.elsevier.com/locate/jnucmat

The fracture strength of TRISO-coated particles determined by compression testing between soft aluminium anvils

Gerrit T. van Rooyen *, Rudy du Preez, Johan de Villiers, Robert Cromarty

Department of Materials Science and Metallurgical Engineering, University of Pretoria, South Africa

ARTICLE INFO

Article history:
Received 10 December 2009
Accepted 4 June 2010

ABSTRACT

Compression testing of tri-isotropic (TRISO) carbon/silicon carbide-coated fuel particles between anvil materials with a wide range of hardnesses was investigated. During compression testing, the particle produces a hardness impression before it fractures. For subsequent measurements, the same position can therefore not be used.

A special testing machine was designed to use the same set of anvils for testing more than one specimen. By each time positioning a particle at a slightly different position between the anvils, a large number of measurements could be made. The load required for fracture is almost independent of anvil hardness for very hard or very soft anvils. Finite element stress analysis showed that when the anvil hardness is very high, fracture occurs because of high local contact bending stresses at the point of contact.

In the case of very soft anvils, a tensile stress develops along a latitudinal direction along the perimeter of the particle over a large volume in between the contact zones with the anvils. The particle then fractures by the development of cracks at right angles to the direction of the tensile stress. From the fracture load, the ability of the particle to withstand internal pressure can be assessed. The advantages of using compression testing of full particles between soft anvils without prior preparation to complement previous test methods are highlighted.

1. Introduction

The silicon carbide (SiC) layer in TRISO-coated particles used in the Pebble Bed Modular Reactor (PBMR) has the function of containing the radioactive fission products within the particle. Gaseous fission products, together with carbon monoxide, trapped within the particles, develop a significant pressure. The pressure results in a uniform biaxial tensile stress (σ) in the particle. The sum of the applied stress σ due to internal pressurisation and any residual stress present has to be less than the fracture stress (σ_f) to ensure that the particle does not fail. Several techniques have been used to establish the fracture stress of the SiC shell [1–8]. Apart from full particle testing, some of the techniques involve the sectioning of a particle and removing the surrounding pyro carbon (PyC) before fracturing the specimen. In this way, the strength of the SiC intermediate layer is determined rather than that of the combination. Evaluating the contribution of residual stress and the presence of pyro PyC layers to the strength are also important and can only be assessed by full particles testing [9,10]. Apart from full particle compression of TRISO particles between anvils, most of the other techniques require very careful specimen preparation and are not amenable for testing very large batches of particles or of particles after irradiation.

SiC is a brittle ceramic and the fracture strength is determined by the presence of defects both internal and external. Fracture of a uniformly stressed specimen usually starts at the defect where the local stress due to the presence of stress raisers due to surface roughness and cracks is the largest, that is, where the applied stress intensity is the largest. Without defects, the fracture strength should approach the theoretical strength of about 40 GPa [11]. With defects, the strength depends on the fracture toughness of the material and fracture occurs where the local stress intensity reaches the fracture toughness value. Statistically, the probability of a severe stress raiser being present depends on the volume of stressed material. Fracture stress would therefore also depend on the volume of material stressed. Compression testing of a ring or a hemispherical-shaped SiC specimen shaped between very hard anvils produces an almost point contact between the particle and the anvil. This results in a very small conical volume of highly stressed material. The SiC shell at the point of contact is subjected to a bending stress such that the outer surface is compressed and the inner surface elongated. The volume of material subjected to high tensile stresses can be increased by using a thin softer insert between the SiC and the hard anvil [12–14]. This produces a small, almost uniformly highly stressed zone where the stress can be obtained by using finite element analysis (FEA) [14]. Due to the small volume of SiC under tension, the fracture stress thus calculated when the particle fails would not be representative of the bulk properties. By using statistical

* Corresponding author. Tel.: +27 12 420 3190.
E-mail address: gerrit.vanrooyen@up.ac.za (G.T. van Rooyen).

0022-3115/$ - see front matter © 2010 Elsevier B.V. All rights reserved.
doi:10.1016/j.jnucmat.2010.06.011

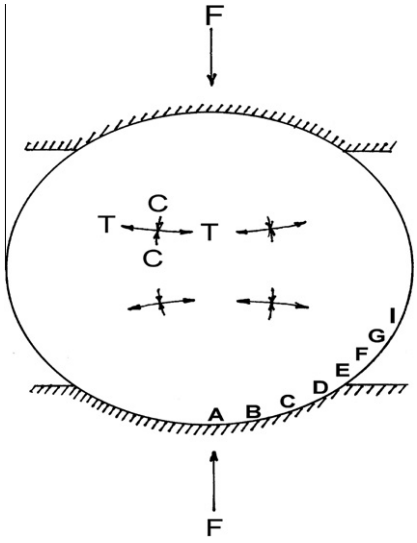

Fig. 1. Schematic that illustrates the development of latitudinal tensile stresses due to compression testing particles between soft anvils (T = tension and C = compression).

measures, it is possible to convert, the measured strength to a value that would be applicable to the whole SiC shell. So far, compression of a full SiC shell between thick very soft anvils by FEA has not been investigated. With very soft anvils, a large indentation is produced. During compression, the initial tensile stress at the contact zone is replaced by compressive stresses and high tensile stresses are generated in a circular volume of material in between the anvils. Depending on the hardness of the anvils, the tensile stress in this volume will be higher than the maximum tensile stress at the initial contact zone.

2. Finite element analysis (FEA)

2.1. FEA model

Compression testing of a spherical shell between soft anvils results in it deforming elastically into a slightly disk shaped object as shown exaggerated in Fig. 1. This result in tensile stresses developing along the girth of the shell as indicated in Fig. 1. FEA modelling was used to quantify the stresses to which a SiC shell is subjected to during compression between soft anvils. Fig. 2[1] shows a quarter of the model where the stress at a specific position is indicated by the colour scale on the right hand side of the figure. The modelling shown applies to a SiC shell with an outer diameter of 800 μm, a shell thickness of 30 μm and aluminium anvils with a yield stress of 80 MPa with no friction between the shell and the anvil. Very similar results but with slightly higher stresses were obtained with a friction coefficient of 0.4. The modelling (Fig. 2) showed that at the stage when FEA was terminated, a maximum tensile stress of 988 MPa is applied to the shell some distance above the point where the shell contacted the anvil. Under favourable conditions up to half of the volume of the shell is subjected to tensile stress within 75% of the maximum value. The direction of this stress is in a direction along a latitudinal direction or normal to the plane of Fig. 1. The tensile stress is almost the same throughout the thickness of the shell. In the longitudinal direction (vertical in Fig. 1), the stress is compressive. In the thickness direction, the stress is essentially zero. Although the stress system generated by compression between very soft anvils is not identical to that due to internal pressurisation, the conditions required for fracture of a brittle material such as SiC are closely simulated.

[1] For interpretation of color in Fig. 2, the reader is referred to the web version of this article.

2.2. Results of the modelling

Fig. 3 shows how the tensile stresses applied at various points along the contour of the hollow shell vary during compression between anvils with a yield stress of 80 MPa. Position A (element 776) is situated directly above the point of initial contact on the inner surface, B at the outer point of contact whereas the positions C, D, E, F, G, H and I are points along the outer surface extending from the initial point of contact upwards as shown in Fig. 1. Curve A shows that a high tensile contact stress develops shortly after contact with the anvil. With further compression, the contact stress decreases again and becomes compressive. At position A on the inside of the shell and directly opposite the point of initial contact, the maximum tensile stress applied (700 MPa at a load of 4 N in Fig. 3) is dependent on the hardness of the anvils used. At a load 40 N the tensile stress in the shell will be 990 MPa. Fig. 4 shows, the development of stress at position A in Fig. 1 when the anvil yield stress is 1000 MPa. At the same load of 40 N the tensile contact stress is now 7600 MPa. FEA analyses show that the maximum contact stress is linearly related to the yield stress of the anvil material.

At a point B directly below point A in Fig. 1 on the outer surface of the shell, the stress is mainly compressive throughout the whole process. During compression, the stress values at the points on the outer surface (C, D, E, etc.) initially rises slower than that at position A, but depending on the hardness of the anvils, will exceed the maximum value at point A. Stresses along the contour of the shell are initially tensile but on coming in contact with the anvil becomes compressive again. If the fracture stress of the shell is constant and not dependent on defects, a shell with a fracture stress less than 700 MPa will fracture when the contact stress reaches the fracture value. Particles with a fracture strength exceeding 700 MPa will survive the initial contact stress and only fracture when the latitudinal stress becomes high enough. If the particle fails at a load of say 40 N in Fig. 3, a tensile stress of 990 MPa is applied to an element in the zone G. The stress in the zone G at this stage of the testing will then be higher than that at any of the other zones. If the shell fails at a load of 40 N and the fracture initiated anywhere along a latitudinal zone corresponding to zone G, the fracture stress of the shell can then be equated to 990 MPa. A line following the outline (outer boundary) of the curves in Fig. 3 can be used to convert the load at fracture to the fracture strength of the SiC shell. If, however, the fracture originated at any other zone due to the presence of a larger defect, and therefore higher stress intensity, the local stress to cause fracture of the SiC would be less than 990 MPa. In the case of real SiC shell where the load at fracture is dependent on the point where the stress intensity at a defect is the highest, the shell may survive the initial high contact stresses and still fail at a latitudinal tensile stress less than 700 MPa. This is because the volume of material subjected to high contact stresses is small and the presence of large defects unlikely.

Values of fracture strength obtained from Fig. 3 will have to be corrected for actual SiC thickness and shell diameter. For a thin walled shell subjected to an internal pressure (p), a diameter (d) and shell thickness of (t), the circumferential stress (σ) will be approximately be $\sigma = \frac{d}{4t} \cdot p$. A similar relationship also applies to the circumferential stress generated during the compression of a SiC shell between soft platens and the load required for fracture. Stress values determined from Fig. 3 for the same load can consequently be corrected for differing SiC shell thickness (t) and the shell diameter (d) using the following

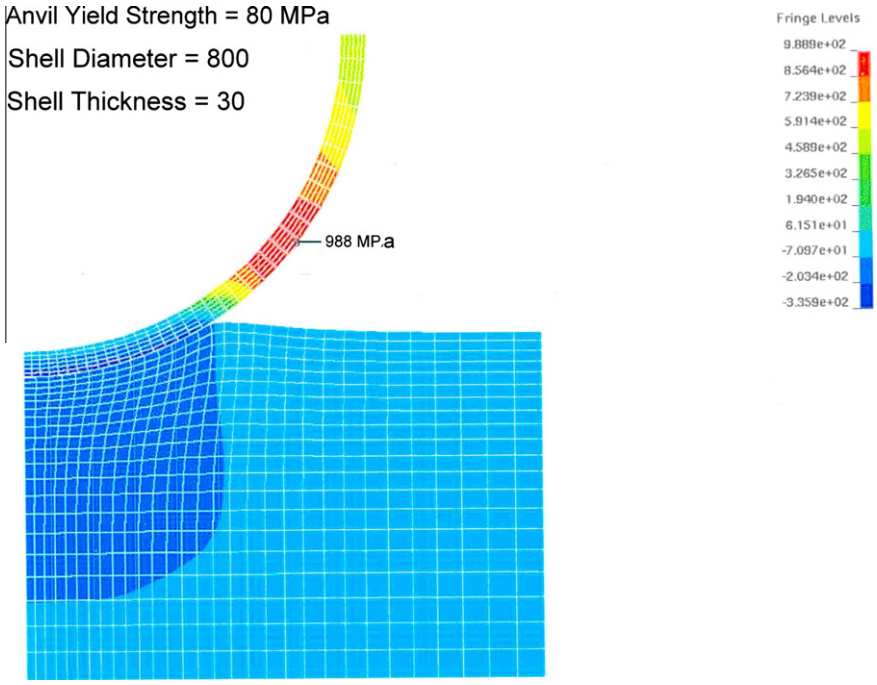

Fig. 2. Finite element model used to determine the stress distribution in the SiC shell during compression testing between thick soft anvils (anvil yield strength = 80 MPa).

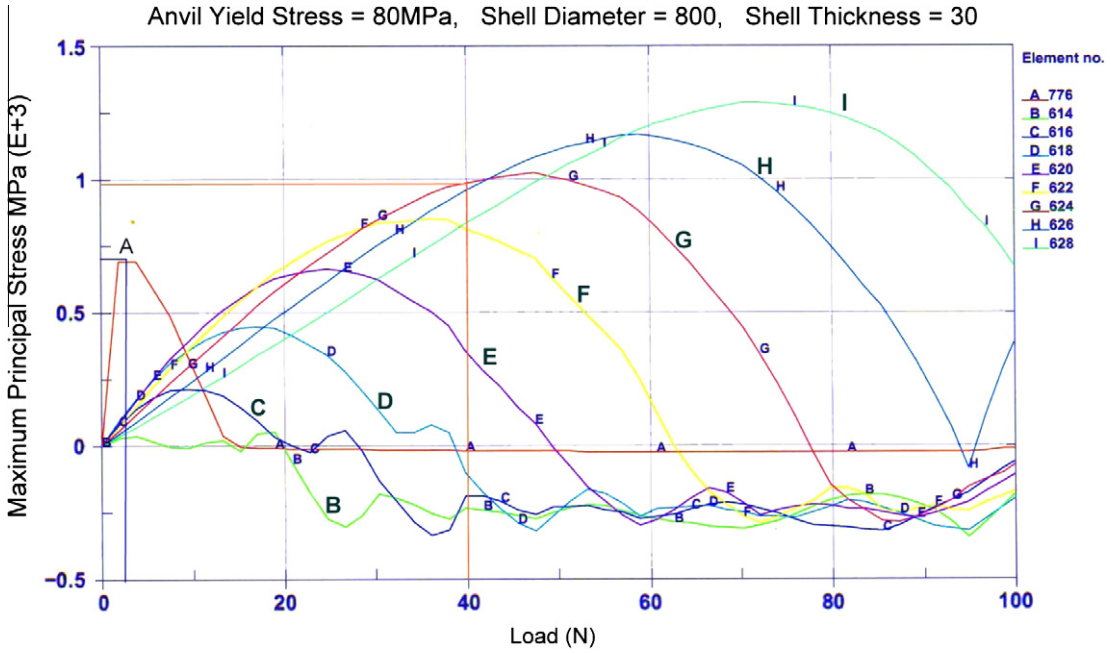

Fig. 3. Stress development at various points on the outside of the shell during compression testing between anvils with yield strength of 80 MPa.

formula: $\sigma_{\text{effective}} = \sigma_{\text{graph}}\left(\frac{30d}{800t}\right)$ where 30 and 800 is the thickness and diameter in μm respectively of the shell used in the FEA model. In the case of compressing a full particle rather than a shell, the stress to fracture will be influenced by the presence of residual stresses and the surrounding PyC carbon layers. The fracture stress values derived from Fig. 3 during full particle testing will therefore not be that of the SiC shell only. However, the load to fracture a particle correctly reflects the ability of the particle to withstand internal pressure independent of the thickness and the diameter of the shell and the contribution by the PyC layers. Apart from thickness, the contribution of the inner and outer layers of PyC to the total strength is influenced by the ratio of the elastic modulus of the PyC to that of SiC and the presence of residual stresses. During compression, with no de-bonding between the SiC and the surrounding PyC, the strain in the pyro carbon and the SiC will approximately be the same. The stress in the PyC and consequently the contribution to the strength of the particle will be much less than that of the SiC. This is because the elastic modulus of the PyC is only about 5% of that of SiC. A calculation shows the actual stress applied to the SiC shell in a particle is about 15–20% less than that derived from shell in Fig. 3. The actual stress at which the SiC shell in a particle fractures will always be the stress applied

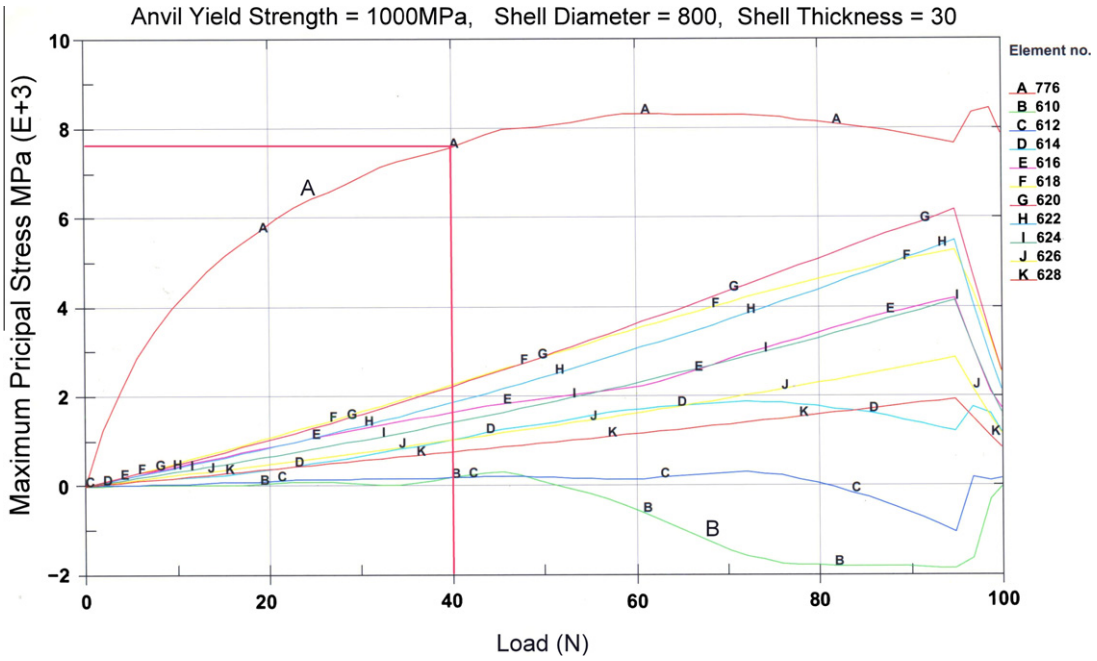

Fig. 4. Stress development at various points on the outside of the shell during compression testing between anvils with yield strength of 1000 MPa.

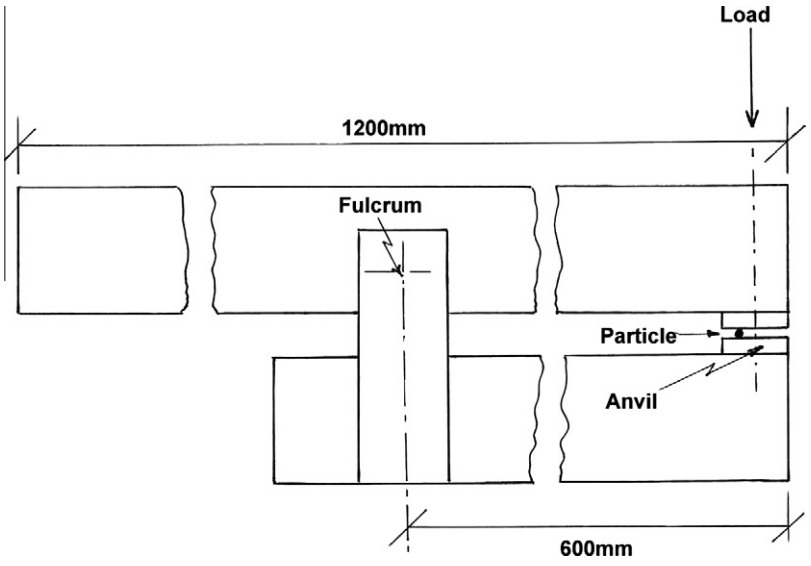

Fig. 5. Schematic drawing of the testing machine.

during compression testing plus that due to the presence of residual stress. However, by compression testing between soft anvils a much larger volume of material is subjected to tensile loading than is the case for very hard anvils and the strength values more representative of the bulk properties of TRISO particles.

Table 1
Average thickness of the SiC and PyC layers of the TRISO particles tested.

Batch	Buffer layer (μm)	Inner PyC layer (μm)	SiC layer (μm)	Outer PyC layer (μm)
A	112	64	32	48
B	113	72	39	48

3. Experimental apparatus

For testing the strength of TRISO particles, a testing machine shown schematically in Fig. 5 was designed and constructed. The movement of the two anvils were constrained by two solid steel bars pivoted at a distance of 600 mm from the position where the anvils (16 × 16 mm) were fixed. This allowed an almost parallel movement of the anvils during the ±0.3 mm movement required during testing to fracture a particle. The force applied was measured by a strain gauge load cell connected to a peak holding digital voltmeter. By this arrangement, it was possible to use the same set of anvils by each time positioning a particle at a slightly different new position on the anvil surface. Although the position of the particle and the position where the load was applied do

not always coincide exactly, the difference was never more than 6 mm apart. Due to the difference in the lever arm, the load measured was never more than 6/600 or 1% different from the actual load required for fracturing. Because the measured strength values for a batch of particles could differ by more than a factor of five, no correction for this effect was necessary.

4. Experimental results

Two experimental batches A and B of TRISO particles with zirconia kernels were tested. The relevant properties are shown in Table 1.

The load to fracture each particle is arranged in an ascending order of strength and the results plotted graphically as shown in Fig. 6 for batches A and B as-received. All of the results presented were performed with the outer PyC layer intact. Removing the outer PyC layer by decarburisation at 700 °C gave results comparable to tests performed with the layer of PyC intact. In general, there is a continuous distribution of strength values for a particular set of anvils. The ratio of the highest to the lowest load can be as much as a factor of five. Part of this variation can be accounted for by differences in the diameter and shell thickness of individual particles. However, for a particular batch the shell thickness and the diameter of the particles do not vary that much. The reason for the large variation in strength is probably due to differences in the nature and magnitude of defects in individual particles.

In order to assess the influence of the anvil hardness on the load required to fracture particles, anvil hardnesses ranging from that of annealed pure aluminium (HV = 20) to hardened high-speed steel (HV = 930) were used. Results are shown in Figs. 7 and 8. There is very little influence when either very hard or very soft anvils are used. In the case of very hard anvils, the fracture occurs at low loads because of the very high contact stress at the point of contact. An example of this is shown by the fracture remnants in Fig. 9a where the white phase is that of the SiC shell. In the case of very soft anvils, the fracture is initiated outside the contact zone due to the presence of tensile stress in the latitudinal direction. An example of this is shown in Fig. 9b. In the intermediate range of anvil, hardnesses there are probably an overlapping mode of fracture. The results show that when the hardnesses of the anvils are low enough (HV = 20 and HV = 38) there is no significant difference in the results. This is due to particles fracturing outside area where they are in contact with the anvils. Due to the advantage of testing particles when they do not fracture as a result of contact stresses, soft anvils are preferred and all further testing was done using anvils with a Vickers hardness of HV = 38.

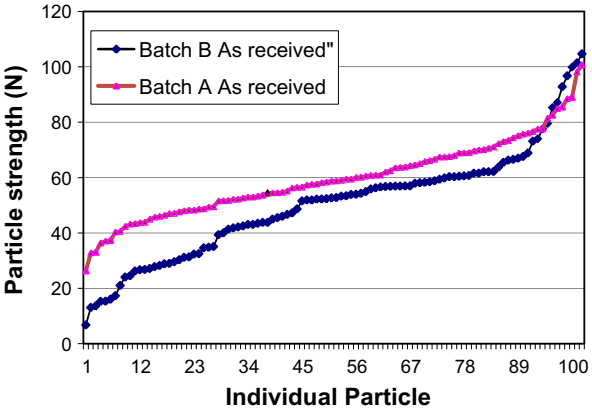

Fig. 6. Comparison of the strength of batches A and B (anvil hardness HV = 38).

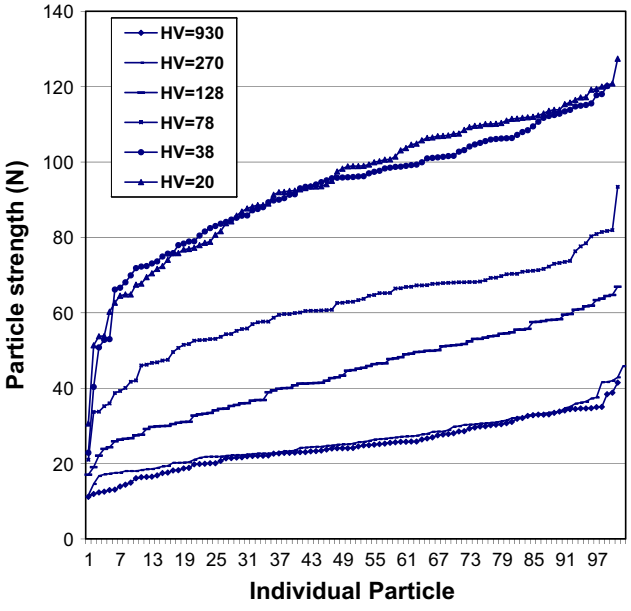

Fig. 7. The influence of anvil hardness on the load to fracture particles. (Batch A heat-treated at 1800 °C for 2 h.)

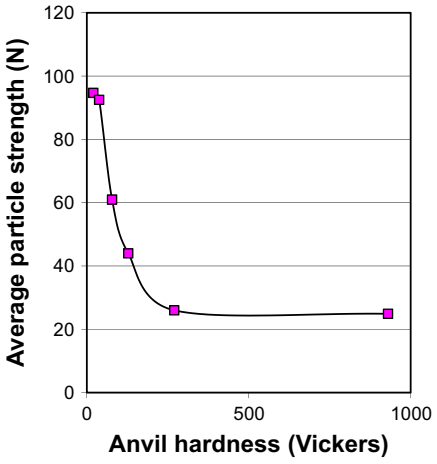

Fig. 8. The influence of anvil hardness on the load required for fracturing. The values refer to particles from batch A after heat-treating at 1800 °C.

TRISO particles are usually consolidated into larger balls, which are then circulated in the pebble bed reactor. In this process, they are subjected to high temperatures approaching 2000 °C. To investigate the influence of this heat cycle, batches of particles were heat-treated at temperatures up to 2000 °C for 2 h in a high temperature carbon furnace. Results of these tests in comparison to the as-received condition are shown in Figs. 10 and 11 for batches A and B respectively. In both cases, there was a considerable improvement in the median strength of the particles. However, the strength of the weakest particles was not improved. This particularly was the case of particles from batch B where the strength of about 20% of the batch was actually slightly lowered by the heat-treatment.

Weibull plots for the data shown in Figs. 7 and 10 are reproduced in Figs. 13 and 14 respectively. Table 2 shows the relevant Weibull constants for the data in Fig. 13.

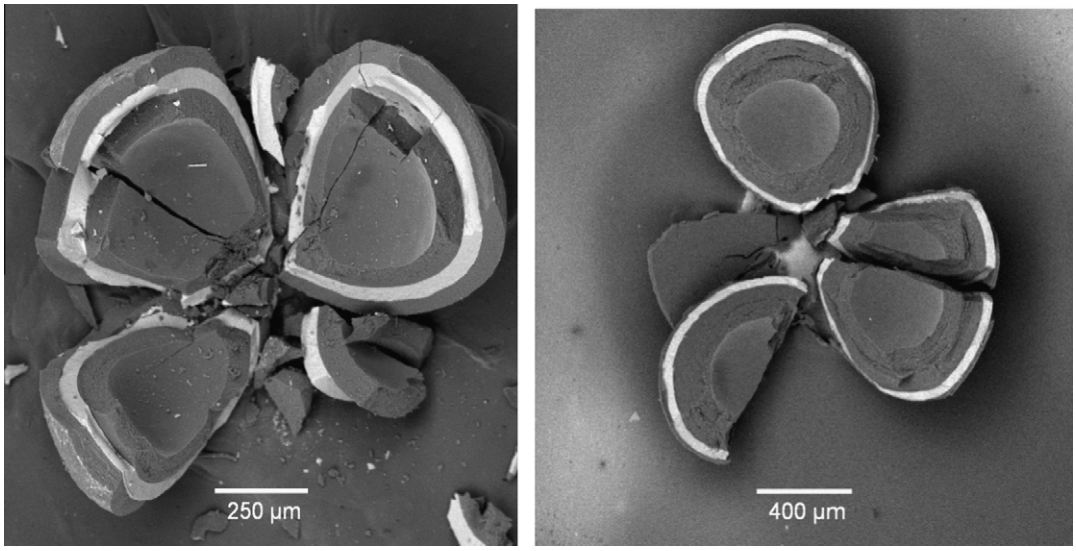

Fig. 9a. Fracture remnants of particles tested between very hard anvils. Note that crack initiation started at the point of contact with the anvil.

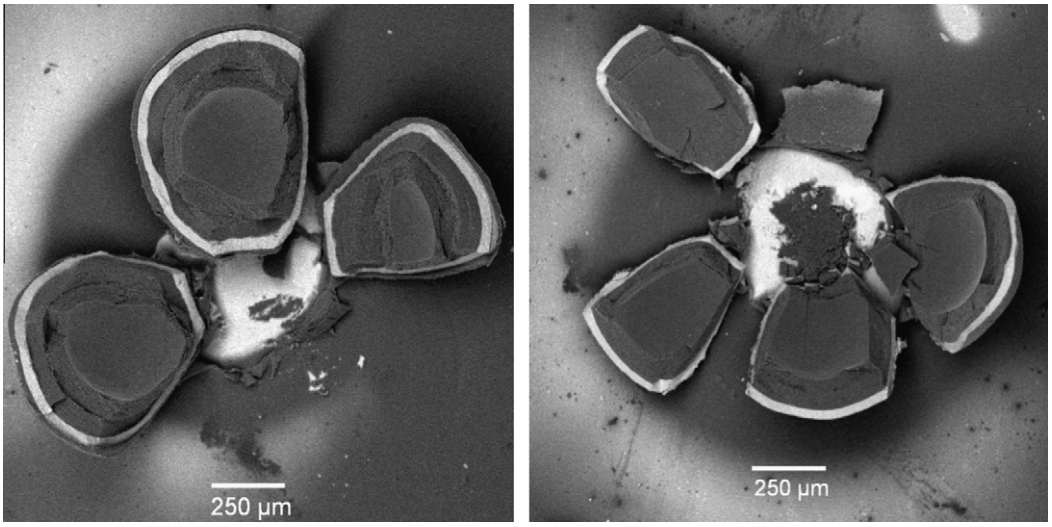

Fig. 9b. Fracture remnants of particles that were tested between soft aluminium anvils (HV = 38). Radial crack initiation started in between the contact zones with the anvils and at right angles to the direction of the applied tensile stress. Note that the SiC at the contact point is not cracked.

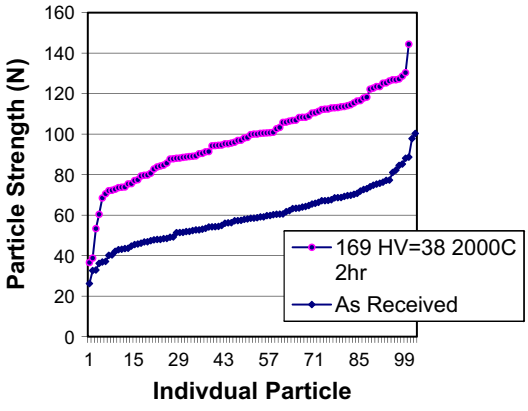

Fig. 10. The influence of heat-treating particles from batch A at 2000 °C for 2 h on the load to fracture. Anvil hardness HV = 38.

5. Discussion

Due to the variations in SiC shell thickness and diameter, some variation in strength can be expected. Actual measurements of shell thickness from fractured particles that failed at low and high loads from the same batch, for example, indicated that there were no significant differences. There were also minor variations in the external diameter of particles. There was, however, no correlation between particle strength and external particle diameter.

The fact that particles fail at low loads when soft anvils are used is not necessarily indicative of fracturing as a result of the initial contact stress, but rather due to the presence of latent cracks elsewhere where the local stress intensity was very high. In rather exceptional instances, it is possible that a very large defect will be at or very close to the initial point of contact with the anvil. Due to the stress concentration effect, such a particle will then fracture at an abnormally low load. This could explain the 3–5 particles (3–5%) in Fig. 10 that failed at abnormally low loads. Failures

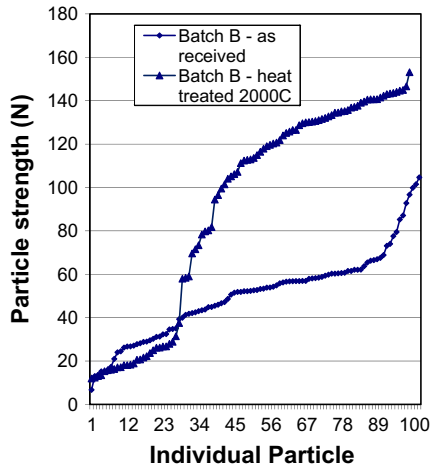

Fig. 11. Influence of heat-treating batch B at 2000 °C on the load to fracture (anvil hardness HV = 38).

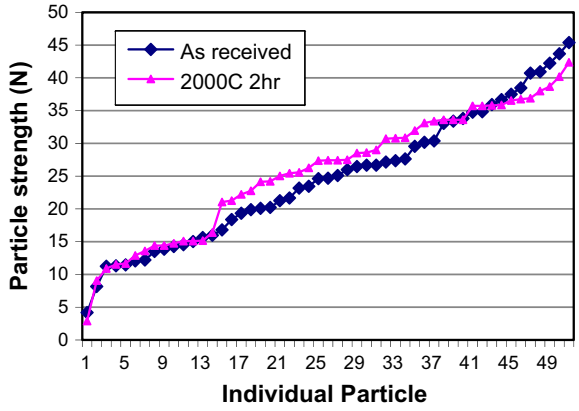

Fig. 12. The influence of heat-treatment at 2000 °C for particles from batch B when very hard anvils (HV = 930) are used during compression testing.

at abnormally low loads are not a feature when very hard anvils are used and where all of the particles fail at the contact zone as indicated in Fig. 10. The abnormal low strength values are also the reason for the deviation of data points from a straight line in the Weibull plots in Figs. 13 and 14. Abnormally low fracture loads when very soft anvils are used are a characteristic of the testing method rather than an indication of inherently weak particles. Of the particles failing at abnormally low loads there may indeed be a few inherently weak particles that do not fail as a result of high contact stress and where the load at fracture is a true indication of their strength. This represents a limitation of the testing method. Inherently very weak particles could probably be identified by using even softer anvil materials. Normal strength particles will then not fracture but become fully imbedded in the softer anvil. By neglecting, the 3–5% data points in the Weibull distribution that deviate from a straight line, the fraction of particles expected to fail at any arbitrary load can, however, be calculated.

One of the salient features when the load to fracture is converted to effective fracture stress is the high values that are obtained. When the average strength of batch A is converted to fracture strength of the SiC shell, an average value of 935 MPa is obtained. This compares with values quoted in the literature that ranges from 670 MPa to 1650 MPa. A direct comparison is, however, not possible because full particle testing also includes the influence of the PyC layers. There is, however, also a difference in the stress system applicable during compression testing in comparison with some of the other testing means. In the conventional testing using rings or hemispherical specimens, mainly bending stresses are applied. In the present case, the principal stress in the longitudinal direction is compressive. For a sphere under internal pressure, two of the principal stresses are tensile (biaxial stress). In the case of brittle materials such as SiC, the main driving force for crack propagation is the maximum tensile stress. Secondary compressive stresses are not considered important. In the present case, the presence of a compressive stress in the longitudinal direction may well have some influence on the results of the tensile strength value reported above.

In all instances, the interface between the SiC and the PyC layers (Fig. 15) was characterised by rough surfaces, which acts as stress raisers. The position of the defect whether on the inside or the out-

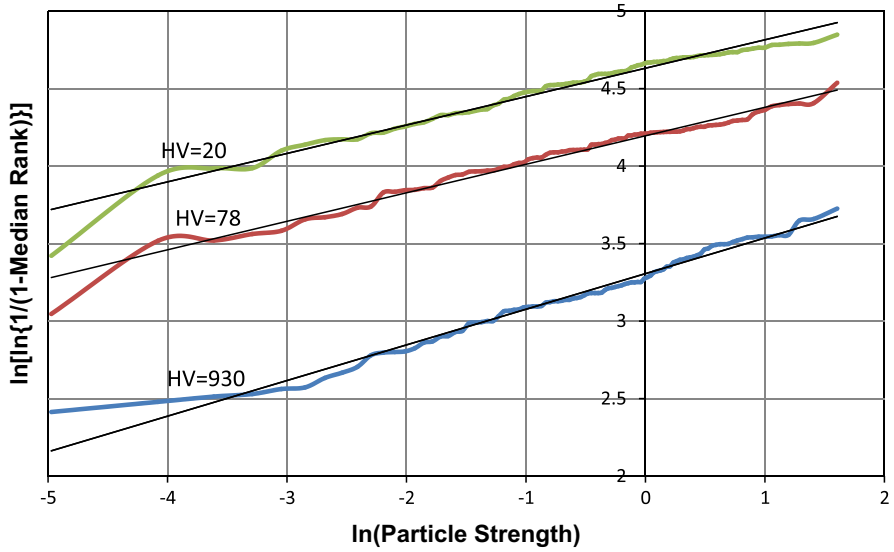

Fig. 13. Weibull plots for different anvil hardnesses from the data shown in Fig. 7.

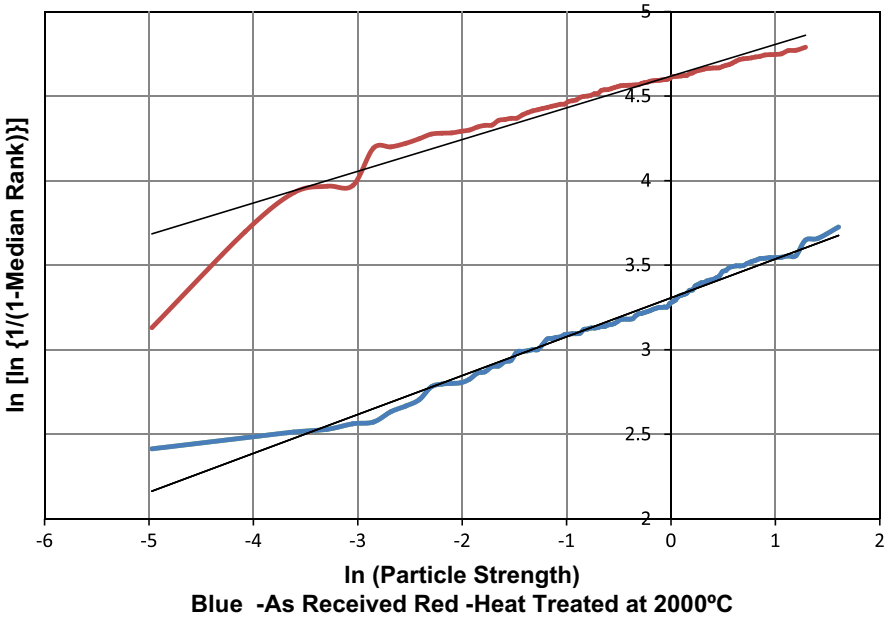

Fig. 14. Weibull plots showing the influence of heat-treatment (data for batch A from Fig. 10).

Table 2
Influence of the anvil hardness on the Weibull constants.

Anvil hardness (Vickers)	Mean strength (N)	Characteristic strength (N)	Weibull modulus (β)
20	92.5	99.1	6.8
78	61.2	66.1	5.8
930	24.5	27.4	4.2

side is immaterial because the tensile stress generated is virtually constant across the thickness of the shell.

An interesting feature is the differences in strength values obtained for the two batches tested. The average strength for batch B as-received was lower than that of A in spite of a thicker shell thickness (39 versus 32 μm) (Table 1). However, after heat-treatment, the situation was reversed where the strength of the "strong" particles of batch B was higher than that of batch A (Figs. 10 and 11). It is, for example, probable that the coating temperature for the two batches as manufactured was different and that this factor was eliminated by the subsequent heat-treatment at the same but higher temperature. To determine the quality of a batch of TRISO particles, it is therefore advisable to heat-treat particles at the temperature to which they will be subjected during the subsequent treatment used for consolidation into larger balls, before testing. The reason for the improvement in the fracture strength by a high temperature heat-treatment requires further investigation. A high temperature heat-treatment can for example result in densification, stress relief of residual stress or an increase in the fracture toughness of the SiC shell. It is also possible that the heat-treatment effect on strength is related to processing conditions during coating and that the strengthening in the experimental batches tested may not necessary always be present. An examination of the fracture surfaces of remnants by electron microscopy did not reveal differences between particles that fractured at respectively low or high loads. Neither were there very noticeable differences after heat-treating at 2000 °C. Fig. 16a and b show typical high magnification photographs of fracture surfaces due to cleavage. All of the fracture surfaces show extensive twin boundaries. By comparing Figs. 11 and 12 it is clear that the

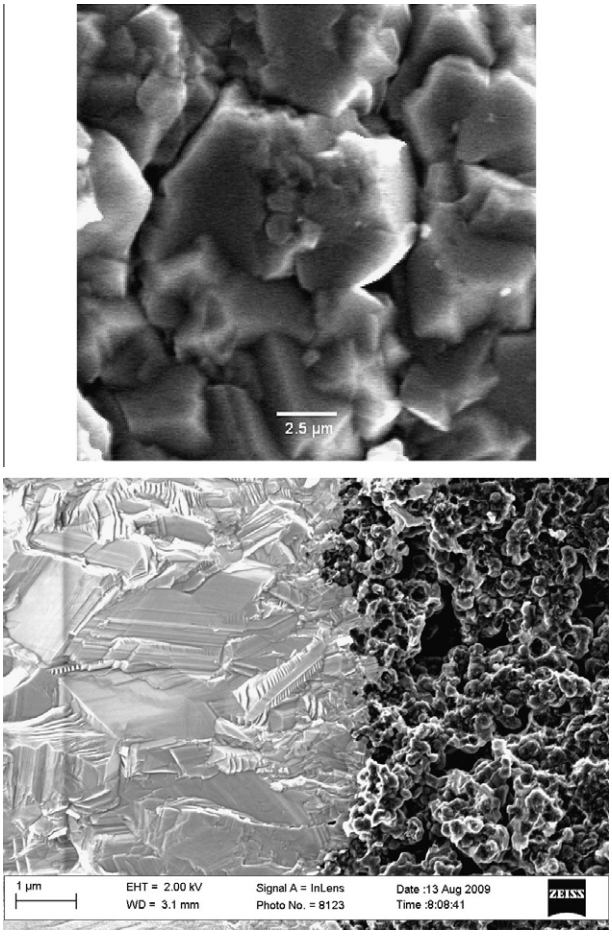

Fig. 15. Photographs showing the SiC surface and interface between the pyrolytic carbon and the SiC respectively.

increase in strength due to a high temperature treatment is not reflected when very hard anvils are used. This is because the volume of material subjected to high stresses is very small and

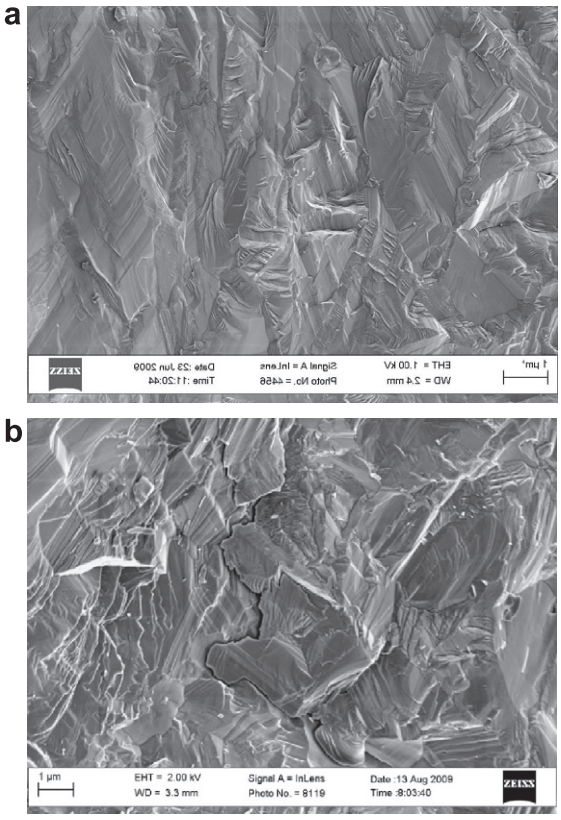

Fig. 16. (a) Sample A (as-received), (b) sample A (heat-treated). Photographs of the fracture surface of the SiC shell. Fracture occurred by cleavage. Note the extensive twinned planes.

not representative of the bulk properties. This clearly shows the value of using relatively soft rather than hard anvils in compression testing to evaluate the mechanical properties of TRISO particles. The fact that no specimen preparation is required is an advantage, particularly when particles after irradiation have to be tested. Any internal gas pressure due to irradiation or the presence of residual stress will add or subtract to the stress applied by compression testing between soft anvils and consequently affect the load at fracture.

6. Conclusions

The finite element analysis and the experimental results have shown that full particle testing between very soft anvils complements the other techniques, which have so far been employed to assess the strength and integrity of TRISO particles. The advantage of using soft anvils rather than hard anvils has been highlighted. The method has the advantage that a large volume of the particle is subjected to tensile stresses and that no specimen preparation is required. By testing, the whole particle rather than only the SiC shell, the influence of the pyro carbon layers and residual stresses are also included. The method is consequently imminently suitable as a quality control instrument. Because no specimen preparation is required strength measurements on irradiated samples is possible, if provided with a suitable environment. All things remaining the same, the reduction in the load required to fracture a particle subjected to internal pressure is independent of the diameter or the thickness of the SiC shell and the decrease in strength a direct measure of the magnitude of the internal pressure.

Acknowledgments

The authors wish to express their thank to the Pebble Bed Modular Reactor (Propriety) Limited, South Africa for its financial support and for the experimental batches of TRISO particles received.

References

[1] W.J. Kackey, D.P. Stinton, R.L. Beatty, Nucl. Technol. 31 (1976) 191–201.
[2] A. Griggs, R.W. Davidge, C. Pagett, S. Quickenden, J. Nucl. Mater. 61 (1976) 233–242.
[3] K.E. Gilchrist, J.E. Brocklehurst, J. Nucl. Mater. 43 (1972) 347–350.
[4] T. Ogawa, K. Ikawa, J. Nucl. Mater. 98 (1981) 18–26.
[5] G.K. Miller, D.A. Petti, J.T. Maki, J. Nucl. Mater. 334 (2004) 79–89.
[6] L.L. Snead, J. Nucl. Mater. 371 (2007) 329–377.
[7] X. Zhao, R.M. Langford, T. Tan, P. Xiao, Scripta Mater. 59 (2008) 39–42.
[8] K. Minato, K. Fukuda, K. Ikawa, J. Nucl. Sci. Technol. 19 (1982) 69–77.
[9] Y.M. Lu, I.C. Leu, Thin Solid Films 378 (2000) 389–393.
[10] K. Niihara, Am. Ceram. Bull. 63 (1984) 1160–1164.
[11] R.W. Hertzberg, Deformation and Fracture Mechanics of Engineering Materials, John Wiley and Sons Inc., 1996, pp. 264–265.
[12] T.S. Byun, J.D. Hunn, J.H. Miller, L.L. Snead, J.W. Kim, Int. J. Appl. Ceram. Technol. 11 (11) (2009) 1–11.
[13] S.G. Hong, T.S. Byun, R.A. Lowden, L.L. Snead, Y. Katoh, J. Am. Ceram. Soc. 90 (2007) 184–191.
[14] J.W. Kim, T.S. Byun, Y. Katoh, Ceram. Nucl. Appl. 10 (2009) 149–159.